PROCEEDINGS OF SCIENCE

Higgs boson differential cross section measurements and effective field theory interpretation with CMS experiment

Suman Chatterjee *
on behalf of the CMS Collaboration

Institute of High Energy Physics (HEPHY), Austrian Academy of Sciences (ÖAW), Nikolsdorfer Gasse 18, 1050 Vienna, Austria

E-mail: suman.chatterjee@cern.ch

Since the discovery of the Higgs boson in 2012, the precise determination of its properties and interaction with other particles remains a central focus of research at the CERN LHC. Differential cross section measurements of variables characterizing the Higgs boson across a number of its decay modes are performed, scrutinizing the theoretical modeling across a broad range of kinematic spectra as well as probing for the presence of physics beyond the standard model. Sophisticated observables are developed to probe the potential presence of new physics at energy scales higher than those directly accessible at the LHC, modifying the Higgs boson coupling to other fundamental particles. A number of results, public as of June 2024, reporting differential measurements and searches for the effect of effective field theory operators using 138 fb^{-1} of data collected by the CMS experiment in proton-proton collisions at a center-of-mass energy of 13 TeV is presented.

12th Large Hadron Collider Physics Conference (LHCP2024)
3-7 June 2024
Boston, USA

*Speaker

PoS(LHCP2024)126

1. Introduction

Since the discovery of the Higgs boson (H) in 2012 [1–3], extensive measurements at the CERN LHC have been performed to pin down the nature of its properties and interaction with other fundamental particles scrutinizing the predictions of the standard model (SM) of particle physics as well as looking for possible signatures of physics beyond the SM (BSM). New physics, if present, can induce anomalous couplings of the H boson, which can also be interpreted as the effects of higher-dimensional operators involving SM fields and satisfying SM gauge symmetries that extend the SM Lagrangian in an effective field theory (EFT) framework. In the following, results of a number of differential cross section measurements targeting various H production modes and analyses designed to probe EFT effects are reported. All results presented in this note use 138 fb^{-1} of data collected by the CMS experiment [4, 5] in proton-proton collisions at a center-of-mass energy of 13 TeV.

2. Measurements of differential cross sections

A set of single- and double-differential cross section measurements is performed as a function of several kinematic variables characterizing H production and decay using the $\text{H} \to \text{W}^+\text{W}^{-(*)} \to \text{e}^\pm\mu^\mp\nu_\text{l}\bar{\nu}_\text{l}$ [6], $\text{H} \to \gamma\gamma$ [7], and $\text{H} \to \text{ZZ}^{(*)} \to 4\ell$ [8] final states within fiducial phase space volumes. The result of a double-differential cross section measurement in the $\text{H} \to \gamma\gamma$ channel is shown in Fig. 1 (left). In the $\text{H} \to \text{ZZ}^{(*)} \to 4\ell$ final state, measurements are also reported as a function of various angular variables characterizing the H decay, as shown in Fig. 1 (right), as well as matrix element discriminants sensitive to anomalous couplings of the H to electroweak vector bosons (V, V = W, Z). Fiducial cross sections of H production are also measured in the $\text{H} \to \tau^+\tau^-$ final state as a function of H transverse momentum (p_T) and jet multiplicity targeting the topologies where the two τ leptons are well separated [9], i.e., resolved topology, or produced spatially close, with overlapping decay products, referred to as the boosted topology. In the latter case, a dedicated algorithm is designed for the reconstruction and identification of hadronic τ decay [10]. Results of both $\text{H} \to \tau^+\tau^-$ analyses are shown in Fig. 2. Measured differential cross sections are compared to theoretical predictions obtained using various generators for modeling the H production via gluon fusion (ggF), the dominant mode for H production.

The $\text{H} \to \text{b}\bar{\text{b}}$ decay, which has the largest branching fraction, is leveraged for detailed measurements of rarer H production modes, as discussed in the following. The cross section for Higgs production in association with an electroweak vector boson is measured in the framework of simplified template cross section (STXS) [11, 12]. These measurements are performed in exclusive phase space regions defined by the type and p_T of the V, as well as the number of additional jets, using the leptonic decay modes of V and the $\text{H} \to \text{b}\bar{\text{b}}$ reconstruction using either two small-radius jets originating due to two b quarks or a large-radius jet containing particles from both b quarks [13]. Multivariate techniques are employed to extract the signal, with the results shown in Fig. 3 (left). A search for H production with high p_T (> 450 GeV) via vector boson fusion (VBF) is carried out using large-radius jets identified through jet substructure information [14]. Events are categorized into independent regions targeting both VBF and ggF productions utilizing forward small-radius jets, which are characteristic of VBF production. Signal strength, defined as the ratio of measured

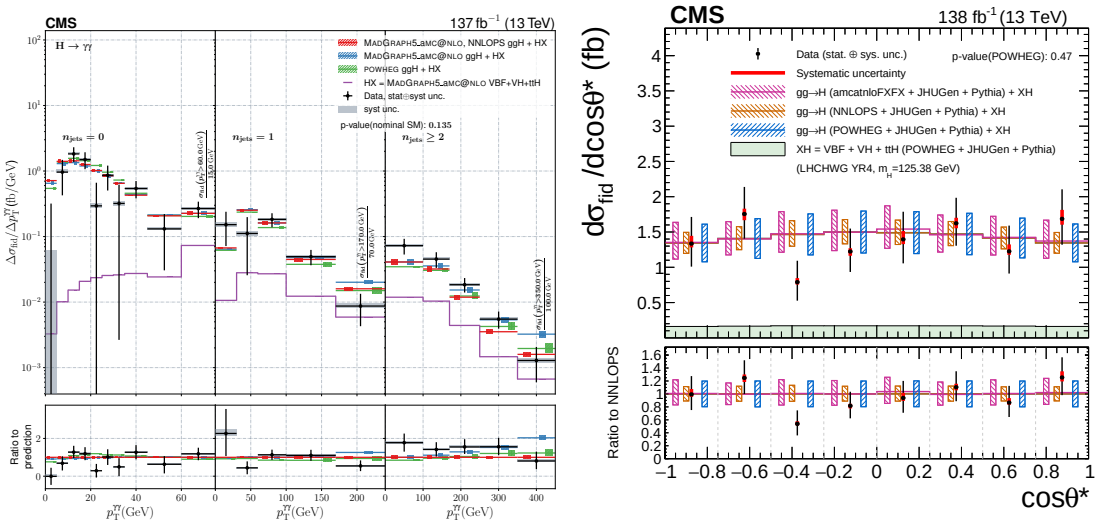

Figure 1: Double-differential cross section in bins of H p_T and number of jets in $H \to \gamma\gamma$ analysis [7] (left). Differential cross section measured in $H \to ZZ^{(*)} \to 4\ell$ analysis as a function of cosine of the angle, defined in the H rest frame, between the beam axis and the direction of one of Z bosons from H [8] (right).

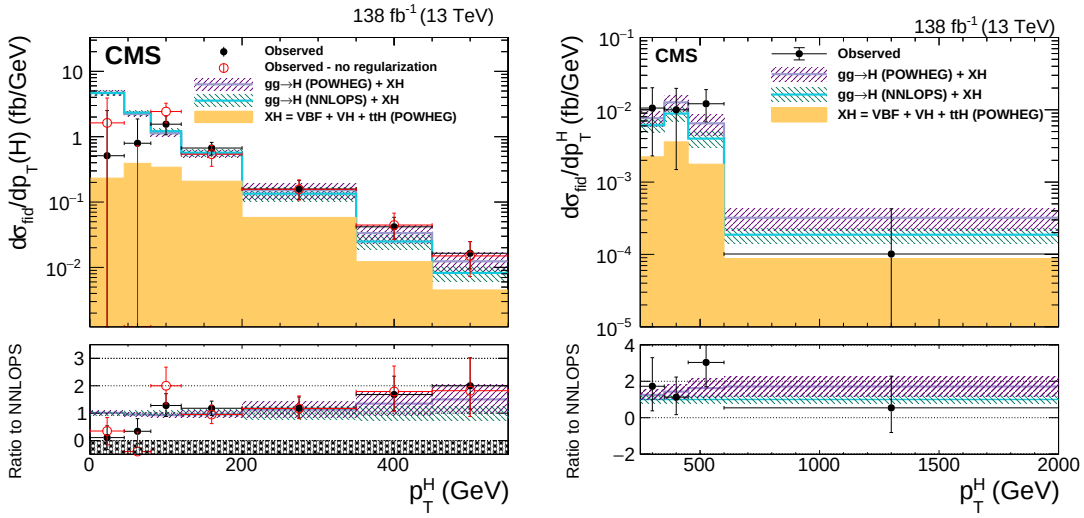

Figure 2: Differential cross section as a function of H p_T in analyses targeting $H \to \tau^+\tau^-$ decay with resolved (left) [9] and boosted [10] (right) topologies.

cross section and SM expectation, is measured at the detector level in two bins of the invariant mass of the forward jets for the VBF category and six bins of the p_T of the H candidate for the ggF category as shown in Fig. 3 (right). The cross section of H production in association with a pair of top quarks (ttH) is measured in different p_T bins of the H candidate within the STXS framework using final states with up to two leptons [15]. The events are categorized by the multiplicity of jets and by the number of those tagged as initiated by b quark(s). The ttH signal is discriminated against backgrounds using artificial neural networks and extracted using a fit to their outputs.

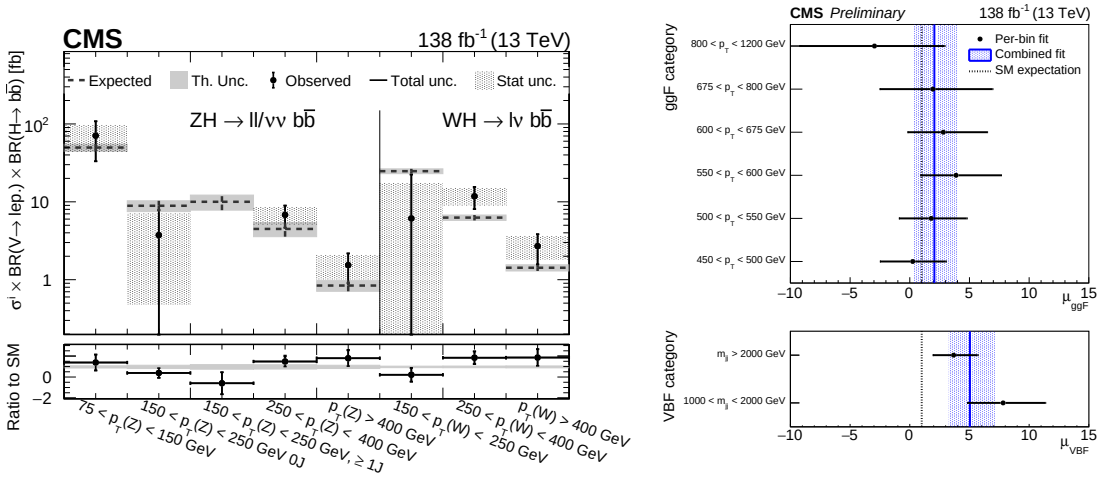

Figure 3: (Left) differential cross section of H production in association with a W/Z boson a function of vector boson p_{T} [13]. (Right) signal strength in bins of H p_{T} for ggF production and invariant mass of forward jets for VBF production [14].

3. Search of effective field theory effects

In this section, the latest results looking for EFT effects in the interaction between H and top quark (t), as well as H coupling to vector bosons of both electroweak and strong interactions, are presented.

3.1 Higgs boson to top quark couplings

The EFT effects modifying the charge-parity (CP) nature of H-t Yukawa coupling are probed using event samples enriched in ttH and H production with a single top quark followed by the $\mathrm{H} \to \mathrm{b\bar{b}}$ decay [15] discussed in the previous section and results are found to be compatible with SM expectations within two standard deviations. A combination of analyses targeting other H decay modes: $\mathrm{H} \to \gamma\gamma$ [16], $\mathrm{H} \to \mathrm{ZZ}^{(*)} \to 4\ell$ [17], and $\mathrm{H} \to \tau^{+}\tau^{-}$ [18], as shown in Fig. 4 (left), provides stronger constraints on the CP structure of the H-t coupling and the pure CP-odd H-t coupling hypothesis is excluded at 3.7 standard deviations. Searches for the effects of multiple dimension-six EFT operators involving H and modifying the H-t coupling as well as giving rise to four-particle interaction are performed in ttH production using Lorentz-boosted H, decaying to a pair of b quarks, exploiting jet substructure techniques to identify the $\mathrm{H} \to \mathrm{b\bar{b}}$ decay [19]. Yields in analysis bins defined using p_{T} and soft-drop mass [20] of the H candidate jet and a deep neural network score separating H or Z production in association with a top quark-antiquark pair from SM backgrounds are used to probe the effects of EFT operators. Results are consistent with SM predictions, and constraints are set on eight operator coefficients by fitting them to data simultaneously or individually. Constraints on the two-dimensional plane of Wilson coefficients corresponding to two operators involving H are shown in Fig. 4 (right).

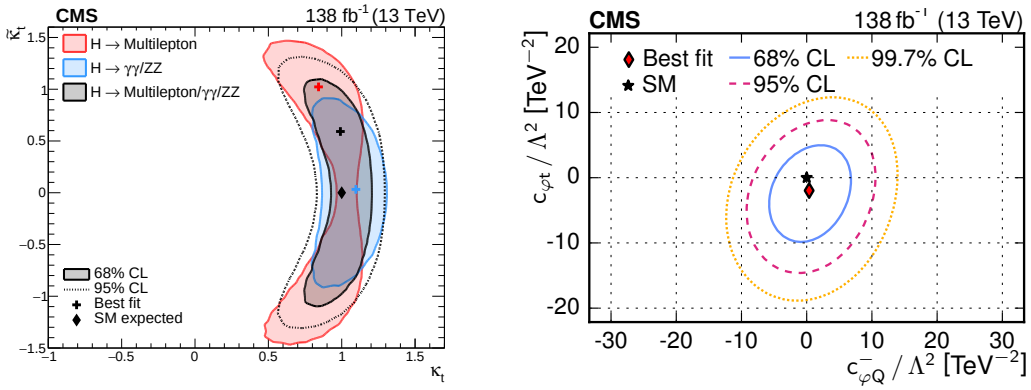

Figure 4: Observed and expected negative log-likelihood scans as functions of CP-even and -odd H-t Yukawa couplings [21] (left) and Wilson coefficients of two dimension-six operators involving H [19] (right).

3.2 Higgs boson to gauge boson couplings

The effects of EFT operators on H to vector boson interactions are probed using an anomalous coupling approach, as discussed in the following. The coupling of H to spin-1 gauge bosons is parameterized by the scattering amplitude:

$$\mathcal{A}(\mathrm{HVV}) \approx \left[a_1 + \frac{\kappa_1^{\mathrm{VV}} q_1^2 + \kappa_2^{\mathrm{VV}} q_2^2}{(\Lambda_1^{\mathrm{VV}})^2} \right] m_{\mathrm{V1}}^2 \epsilon_{\mathrm{V1}}^* \epsilon_{\mathrm{V2}}^* + a_2^{\mathrm{VV}} f_{\mu\nu}^{*(1)} f^{*(2)\mu\nu} + a_3^{\mathrm{VV}} f_{\mu\nu}^{*(1)} \tilde{f}^{*(2)\mu\nu}, \quad (1)$$

where a_1 is an SM-like coupling, κ_1, κ_2, and a_2 are CP-even anomalous couplings, and a_3 is a CP-odd anomalous coupling. For the effective interaction of H with gluon (g), a_1, κ_1, κ_2 are 0 to maintain gauge invariance. Anomalous coupling contributions are probed experimentally by measuring the effective cross section fractions defined as:

$$f_{ai} = \frac{|a_i|^2 \sigma_i}{|a_1|^2 \sigma_1 + |a_2|^2 \sigma_2 + |a_3|^2 \sigma_3 + |\kappa_1|^2 \sigma_{\Lambda 1} + \kappa_2|^2 \sigma_{\Lambda_{Z\gamma}}} \quad . \quad (2)$$

In general, to probe H to gauge boson couplings, one needs multi-dimensional measurements over a large number of observables that fully characterize the system of H production followed by its decay, which is difficult due to the limited volume of data and simulation currently available. This problem is solved using the matrix element likelihood approach (MELA) [22], which takes kinematic variables describing the H production and decay and builds discriminants sensitive to the BSM signature of an anomalous coupling and its interference with other processes, including in the SM. With this approach, one needs to measure a smaller number of observables while retaining most of the information about SM-BSM separation.

The presence of anomalous H to electroweak vector boson couplings is probed in VBF topology with the $\mathrm{H} \to \tau^+\tau^-$ decay [18] as well as using $\mathrm{H} \to \mathrm{ZZ}^{(*)} \to 4\ell$ [17] and $\mathrm{H} \to \mathrm{W}^+\mathrm{W}^{-(*)} \to \mathrm{e}^{\pm}\mu^{\mp}\nu_1\bar{\nu}_1$ [23] final states where EFT effects can be present both in production (via fusion of V's and in association with V) and decay. A set of MELA discriminators is used to distinguish between H production and SM backgrounds, to differentiate various H production modes, as well as to separate the effects of different anomalous couplings. Anomalous couplings are extracted

from multi-dimensional distributions using several MELA variables along with simple kinematic variables, if relevant. Constraints on these couplings are reported under two approaches: approach 1 assumes anomalous H-W and H-Z couplings to be equal, while approach 2 applies SU(2)×U(1) symmetry to relate those. The constraints on anomalous couplings are translated into bounds on sizes of dimension-six EFT operator coefficients in Higgs and Warsaw bases [11, 24]. Constraints on cross section fractions due to CP-even and -odd H-V anomalous couplings derived from the $H \to W^+W^{-(*)} \to e^{\pm}\mu^{\mp}\nu_l\bar{\nu}_l$ analysis and a combination of $H \to ZZ^{(*)} \to 4\ell$ and $H \to \tau^+\tau^-$ analyses are shown in Figs. 5 and 6, respectively.

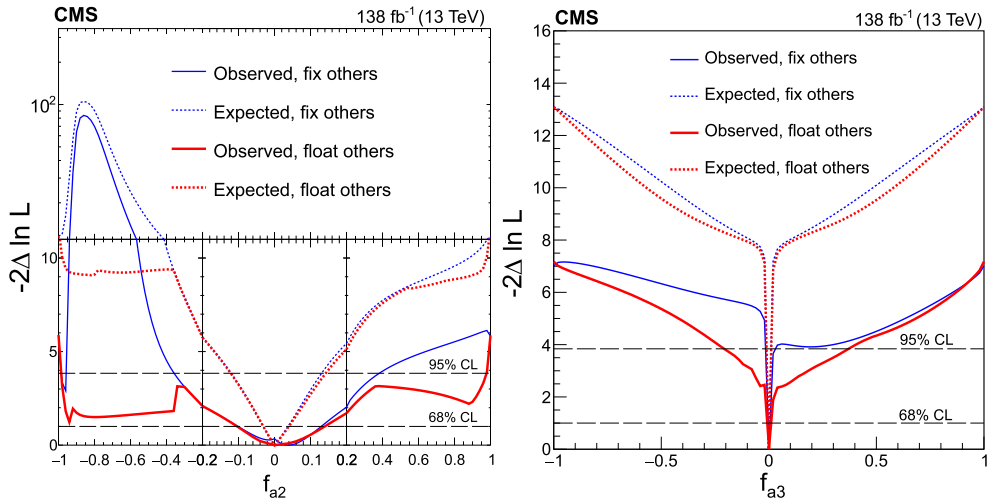

Figure 5: Observed and expected negative log-likelihood scans as function of the cross section fractions of CP-even (left) and CP-odd (right) H-V anomalous couplings from the $H \to W^+W^{-(*)} \to e^{\pm}\mu^{\mp}\nu_l\bar{\nu}_l$ analysis following approach 2 [23].

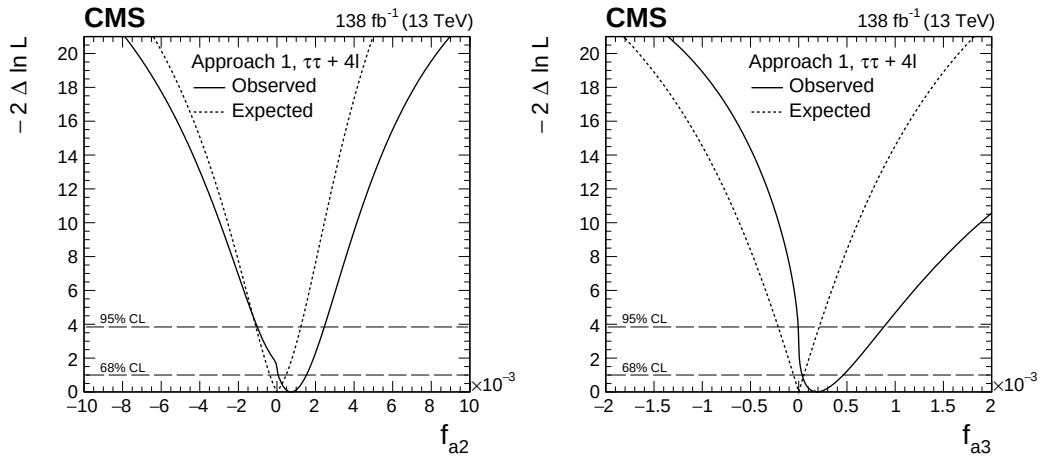

Figure 6: Observed and expected negative log-likelihood scans as function of the fractional cross sections of CP-even (left) and CP-odd (right) H-V anomalous couplings from the combination of $H \to ZZ^{(*)} \to 4\ell$ and $H \to \tau^+\tau^-$ analyses [18] in approach 1.

The presence of a CP-odd anomalous coupling in the effective Higgs-to-gluon vertex is investi-

gated using analyses targeting the $H \to \tau^+\tau^-$ [18], $H \to ZZ^{(*)} \to 4\ell$ [17], and $H \to W^+W^{-(*)} \to e^{\pm}\mu^{\mp}\nu_l\bar{\nu}_l$ [23] final states. Combining the $H \to ZZ^{(*)} \to 4\ell$ and $H \to \tau^+\tau^-$ analyses, the hypothesis of a purely CP-odd H-to-gluon coupling is disfavored by the data at the level of 2.4 standard deviations. In the $H \to W^+W^{-(*)} \to e^{\pm}\mu^{\mp}\nu_l\bar{\nu}_l$ analysis, the observed values of negative log-likelihood gradually exceed the expected ones for larger cross section fractions of the CP-odd H-to-gluon anomalous coupling due to downward statistical fluctuations in the data for a few bins where the effects of this coupling are expected to be significant. Fig. 7 illustrates the constraints on the cross-section fractions for the CP-odd H-g anomalous coupling from the $H \to W^+W^{-(*)} \to e^{\pm}\mu^{\mp}\nu_l\bar{\nu}_l$ analysis (left) and a combination of $H \to ZZ^{(*)} \to 4\ell$ and $H \to \tau^+\tau^-$ analyses (right).

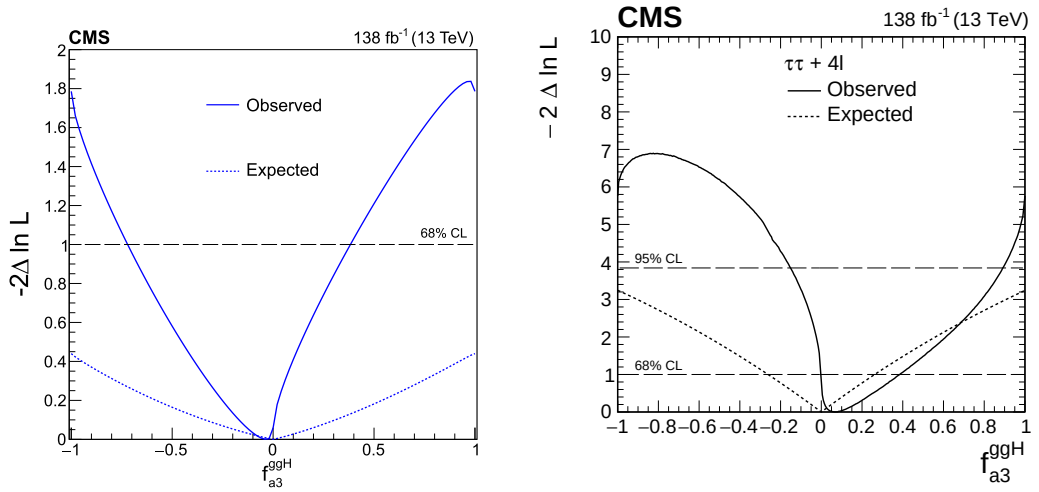

Figure 7: Observed and expected negative log-likelihood scans as function of the cross section fraction of the CP-odd H-gluon anomalous coupling from the $H \to W^+W^{-(*)} \to e^{\pm}\mu^{\mp}\nu_l\bar{\nu}_l$ analysis [23] (left) and the combined $H \to ZZ^{(*)} \to 4\ell$ and $H \to \tau^+\tau^-$ analyses [18] (right).

4. Conclusion

The CMS experiment has performed comprehensive measurements to thoroughly characterize the production and decay of the Higgs boson across a wide range of kinematic spectra using data from Run 2 of the LHC. Studies are also conducted to probe potential signs of new physics at high energy manifesting itself by altering interactions of the Higgs boson with electroweak vector bosons, gluons, and the top quark in the framework of effective field theory. So far, results are found to be in agreement with the predictions of the standard model. While no significant evidence of new physics has been found, our understanding of the Higgs boson has greatly improved thanks to the larger data set and more advanced analysis techniques. Nonetheless, experiments will continue to hunt for any possible signatures of new physics, targeting uncharted territories and exploiting the data from LHC Run 3.

References

[1] ATLAS Collaboration, "Observation of a new particle in the search for the Standard Model Higgs boson with the ATLAS detector at the LHC", *Phys. Lett. B* **716** (2012) 1, doi:10.1016/j.physletb.2012.08.020, arXiv:1207.7214.

[2] CMS Collaboration, "Observation of a New Boson at a Mass of 125 GeV with the CMS Experiment at the LHC", *Phys. Lett. B* **716** (2012) 30, doi:10.1016/j.physletb.2012.08.021, arXiv:1207.7235.

[3] CMS Collaboration, "Observation of a New Boson with Mass Near 125 GeV in *pp* Collisions at $\sqrt{s}$ = 7 and 8 TeV", *JHEP* **06** (2013) 081, doi:10.1007/JHEP06(2013)081, arXiv:1303.4571.

[4] CMS Collaboration, "The CMS experiment at the CERN LHC", *JINST* **3** (2008) S08004, doi:10.1088/1748-0221/3/08/S08004.

[5] CMS Collaboration, "Development of the CMS detector for the CERN LHC Run 3", *JINST* **19** (2024) P05064, doi:10.1088/1748-0221/19/05/P05064.

[6] CMS Collaboration, "Measurement of the inclusive and differential Higgs boson production cross sections in the leptonic WW decay mode at $\sqrt{s}$ = 13 TeV", *JHEP* **03** (2021) 003, doi:10.1007/JHEP03(2021)003, arXiv:2007.01984.

[7] CMS Collaboration, "Measurement of the Higgs boson inclusive and differential fiducial production cross sections in the diphoton decay channel with pp collisions at $\sqrt{s}$ = 13 TeV", *JHEP* **07** (2023) 091, doi:10.1007/JHEP07(2023)091, arXiv:2208.12279.

[8] CMS Collaboration, "Measurements of inclusive and differential cross sections for the Higgs boson production and decay to four-leptons in proton-proton collisions at $\sqrt{s}$ = 13 TeV", *JHEP* **08** (2023) 040, doi:10.1007/JHEP08(2023)040, arXiv:2305.07532.

[9] CMS Collaboration, "Measurement of the inclusive and differential Higgs boson production cross sections in the decay mode to a pair of τ leptons in pp collisions at $\sqrt{s}$ = 13 TeV", *Phys. Rev. Lett.* **128** (2022) 081805, doi:10.1103/PhysRevLett.128.081805, arXiv:2107.11486.

[10] CMS Collaboration, "Measurement of the production cross section of a Higgs boson with large transverse momentum in its Decays to a pair of τ leptons in proton-proton collisions at $\sqrt{s}$ = 13 TeV", arXiv:2403.20201.

[11] LHC Higgs Cross Section Working Group Collaboration, "Handbook of LHC Higgs Cross Sections: 4. Deciphering the Nature of the Higgs Sector", doi:10.23731/CYRM-2017-002, arXiv:1610.07922.

[12] J. R. Andersen et al., "Les Houches 2015: Physics at TeV Colliders Standard Model working group report", in *Proc. 9th Les Houches Workshop on Physics at TeV Colliders (PhysTeV 2015) Les Houches, France, June 1-19, 2015*. 2016. arXiv:1605.04692.

[13] CMS Collaboration, "Measurement of simplified template cross sections of the Higgs boson produced in association with W or Z bosons in the H $\rightarrow$ b$\bar{\text{b}}$ decay channel in proton-proton collisions at $\sqrt{s}$ = 13 TeV", *Phys. Rev. D* **109** (2024) 092011, doi:10.1103/PhysRevD.109.092011, arXiv:2312.07562.

[14] CMS Collaboration, "Search for boosted Higgs bosons produced via vector boson fusion in the $H \rightarrow b\bar{b}$ decay mode using LHC proton-proton collision data at $\sqrt{s}$ = 13 TeV", CMS

Physics Analysis Summary CMS-PAS-HIG-21-020, 2023.

[15] CMS Collaboration, "Measurement of the $t\bar{t}H$ and tH production rates in the $H \to b\bar{b}$ decay channel with 138 fb^{-1} of proton-proton collision data at $\sqrt{s}$ = 13 TeV", CMS Physics Analysis Summary CMS-PAS-HIG-19-011, 2023.

[16] CMS Collaboration, "Measurements of $t\bar{t}H$ Production and the CP Structure of the Yukawa Interaction between the Higgs Boson and Top Quark in the Diphoton Decay Channel", *Phys. Rev. Lett.* **125** (2020) 061801, doi:10.1103/PhysRevLett.125.061801, arXiv:2003.10866.

[17] CMS Collaboration, "Constraints on anomalous Higgs boson couplings to vector bosons and fermions in its production and decay using the four-lepton final state", *Phys. Rev. D* **104** (2021) 052004, doi:10.1103/PhysRevD.104.052004, arXiv:2104.12152.

[18] CMS Collaboration, "Constraints on anomalous Higgs boson couplings to vector bosons and fermions from the production of Higgs bosons using the $\tau\tau$ final state", *Phys. Rev. D* **108** (2023) 032013, doi:10.1103/PhysRevD.108.032013, arXiv:2205.05120.

[19] CMS Collaboration, "Search for new physics using effective field theory in 13 TeV pp collision events that contain a top quark pair and a boosted Z or Higgs boson", *Phys. Rev. D* **108** (2023) 032008, doi:10.1103/PhysRevD.108.032008, arXiv:2208.12837.

[20] A. J. Larkoski, S. Marzani, G. Soyez, and J. Thaler, "Soft Drop", *JHEP* **05** (2014) 146, doi:10.1007/JHEP05(2014)146, arXiv:1402.2657.

[21] CMS Collaboration, "Search for CP violation in ttH and tH production in multilepton channels in proton-proton collisions at $\sqrt{s}$ = 13 TeV", *JHEP* **07** (2023) 092, doi:10.1007/JHEP07(2023)092, arXiv:2208.02686.

[22] A. V. Gritsan, R. Röntsch, M. Schulze, and M. Xiao, "Constraining anomalous Higgs boson couplings to the heavy flavor fermions using matrix element techniques", *Phys. Rev. D* **94** (2016) 055023, doi:10.1103/PhysRevD.94.055023, arXiv:1606.03107.

[23] CMS Collaboration, "Constraints on anomalous Higgs boson couplings from its production and decay using the WW channel in proton–proton collisions at $\sqrt{s}$ = 13 TeV", *Eur. Phys. J. C* **84** (2024) 779, doi:10.1140/epjc/s10052-024-12925-0, arXiv:2403.00657.

[24] B. Grzadkowski, M. Iskrzynski, M. Misiak, and J. Rosiek, "Dimension-Six Terms in the Standard Model Lagrangian", *JHEP* **10** (2010) 085, doi:10.1007/JHEP10(2010)085, arXiv:1008.4884.